Exploring wind energy potential off the California coast

Qingfang Jiang,[1] James D. Doyle,[2] Tracy Haack,[2] Michael J. Dvorak,[3] Cristina L. Archer,[4] and Mark Z. Jacobson[3]

Received 13 May 2008; revised 9 July 2008; accepted 13 August 2008; published 28 October 2008.

[1] Wind energy represents the nearest term cost-effective renewable energy source. While efforts have been made to assess wind energy potential over land around the world, offshore wind energy resources are largely unexplored, in part because these regions have relatively sparse wind observations. In this study, the wind energy potential offshore of the California coast is evaluated using a well-tested high-resolution numerical model dataset. We found that along the coastline, the low-level winds exhibit strong spatial variation and are characterized by alternating windspeed maxima and minima near coastal promontories associated with the interaction between the marine boundary layer and coastal topography. Further analysis highlights the enormous and reliable wind energy development potential in these persistent offshore windspeed maxima. **Citation:** Jiang, Q., J. D. Doyle, T. Haack, M. J. Dvorak, C. L. Archer, and M. Z. Jacobson (2008), Exploring wind energy potential off the California coast, *Geophys. Res. Lett.*, *35*, L20819, doi:10.1029/2008GL034674.

1. Introduction

[2] In recent years, there has been growing interest in taking advantage of strong surface winds to generate electricity, particularly near coastal regions [e.g., *Hasager et al.*, 2005; M. J. Dvorak et al., California offshore wind energy potential, submitted to *Wind Energy*, 2008]. Compared with wind farms over land, offshore wind farms have a number of advantages. Offshore wind turbines pose less threat to wildlife and birds and the rotor noise is likely less of an issue. The size of onshore turbines is often constrained by capacity limitations of transportation and erection equipment. Progressively higher and larger turbines can be installed offshore using powerful marine shipping equipment. In addition, onshore turbines are usually located in remote areas and offshore turbines can operate in sites close to high value coastal load centers, such as populated coastal urban areas, to reduce transmission costs [*Musial and Butterfield*, 2004]. In addition, the low-level windspeed over the ocean is generally larger than over land under similar large-scale flow conditions due to much smaller surface roughness lengths over water. On the negative side, the economic cost and technical requirements for offshore wind turbines are significantly higher, particularly over deeper water. For the existing wind turbine support technology, offshore wind turbines can only be installed over relatively shallow water (50-m or shallower). With emerging technology such as floating turbine support structures, bathymetry issues will become less of a limiting factor. Along the California coast, the coastal population is relatively small adjacent to some of the most promising offshore wind energy resource areas, and public acceptance may be less an issue than in other coastal regions.

[3] It is well known that the instantaneous wind power increases with the cube of the windspeed, and accordingly, a small increase in the windspeed could lead to substantial benefit for wind energy generation. To choose optimal wind farm locations and suitable types of wind turbines, the wind power potential needs to be carefully assessed. Over the past two decades, efforts have been made to map out the wind energy resource potential in the United States [*Elliot and Schwartz*, 1998; *Archer and Jacobson*, 2005]. Two methods are often used to assess the wind power potential based on observational data and high-resolution model data, respectively. An observation-based method constructs the surface wind distribution through horizontal interpolation of surface station measurements. However, the surface station networks are usually insufficiently dense to adequately resolve the rich spatial variations of windspeed that are often present. Numerical modeling approaches require applying well-validated mesoscale models to an area of interest. The model resolution needs to be high enough to adequately resolve land surface features such as topography, which typically plays a significant role in modulating low-level winds. In addition, simulations should cover a relatively long period to make the dataset climatologically meaningful.

[4] In support of several oceanographic field projects, high-resolution numerical simulations have been performed over the past six years using the atmospheric portion of the Coupled Ocean/Atmosphere Mesoscale Prediction System (COAMPS®) [*Hodur*, 1997]. The model dataset consists of three-dimensional wind fields, and in this study is used for assessing wind energy potential off the California coast.

2. Model Description

[5] The atmospheric portion of COAMPS has been applied in a real-time forecast mode since 2003 to provide surface heat and momentum fluxes for quasi-operational ocean models along the California coast. The COAMPS model is a finite-difference approximation to the fully

[1]University Corporation for Atmospheric Research, Naval Research Laboratory, Monterey, California, USA.
[2]Naval Research Laboratory, Monterey, California, USA.
[3]Department of Civil and Environmental Engineering, Stanford University, Stanford, California, USA.
[4]Department of Geological and Environmental Sciences, California State University, Chico, California, USA.

0094-8276/08/2008GL034674$05.00

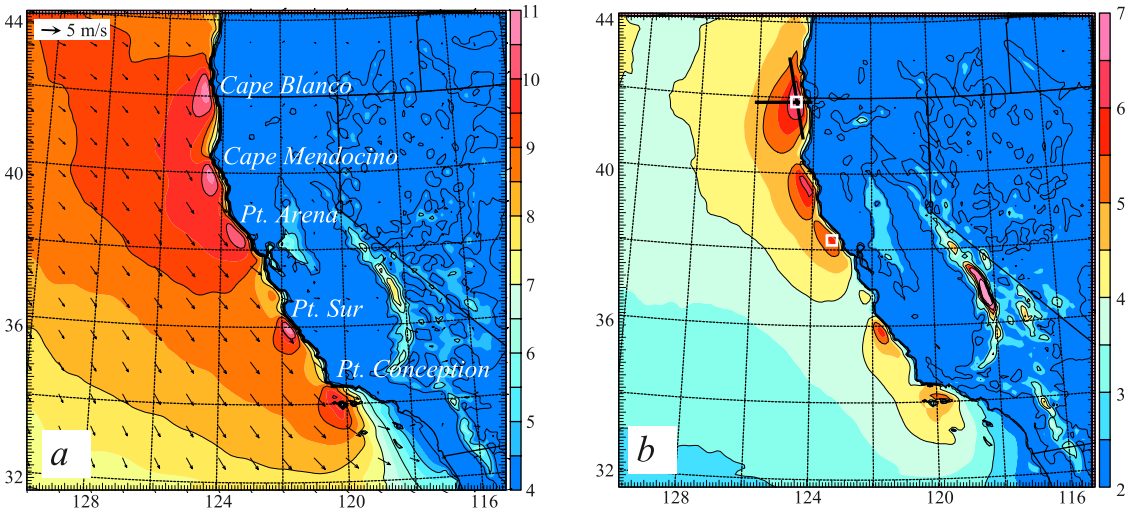

Figure 1. (a) The mean wind speed for 2005 (color, increment: 0.5 m s^{-1}, contour, increment: 1 m s^{-1}) and wind vectors at 90-m AGL. Land areas with elevation above 90 m make use of the windspeed at the lowest model level. Several locations of interest are labeled. (b) The standard deviation (color, increment: 0.5 m s^{-1}, contour, increment: 1 m s^{-1}) is shown. The two white boxes offshore of Cape Blanco and Pt. Arena indicate locations of two hypothetical wind farm sites discussed in Section 4. The bold straight lines indicate the locations of the cross-sections shown in Figure 3.

compressible, nonhydrostatic equations with a suite of physical parameterization options. The initial fields for COAMPS are created from multivariate optimum interpolation analyses of upper-air sounding, surface station, commercial aircraft, and satellite data that are quality controlled and blended with the previous 12-h COAMPS forecast fields. The lateral boundary conditions for the outermost mesh make use of Navy Operational Global Analysis and Prediction System (NOGAPS) forecast fields. The domain configuration for these forecasts contains four horizontally nested grid meshes with grid increments of 81, 27, 9, and 3 km, respectively, centered over central California. The model is configured with 40 vertical levels on a nonuniform vertical grid consisting of an increment of 10 m at the lowest level. The model top is located at 35 km.

[6] COAMPS real-time forecasts and reanalyses over central California have been thoroughly evaluated using buoy and research aircraft observations [e.g., *Haack et al.*, 2001; *Capet et al.*, 2004; *Doyle et al.*, 2008]. In general, the statistical verification of COAMPS forecasts using available observations indicates that COAMPS is very skillful in forecasting low-level winds over this area. In this article, we focus on the spatial and seasonal variation of winds off the California coast in 2005 using the COAMPS data from the 9-km grid, which is comprised of 151 by 151 horizontal grid points and covers the state of California and portions of Nevada and Oregon (Figure 1). A comparison between the annual mean large-scale flow patterns from the COAMPS 27-km grid and the large-scale NCEP GFS reanalysis (not shown) indicates that COAMPS simulations are in agreement with the NCEP GFS reanalysis. An analysis of the NCEP reanalysis between 1985 and 2005 indicates that 2005 is a climatologically typical year. For 2005, we also compared the simulated (forecast period 4–16 h) and buoy measured 10-m winds from 17 NDBC (i.e., NOAA's National Data Buoy Center) buoys within the 9-km domain. The overall agreement is quite reasonable with an average wind speed bias of 1.0 m s^{-1} and RMS error of 2.6 m s^{-1}.

3. Spatial and Seasonal Variation of Offshore Winds

[7] We focus on the spatial and seasonal variation of the windspeed at the 90-m level, motivated by the characteristics of large modern wind turbines. The mean low-level winds offshore of the California coast are influenced by a mean pressure trough off the Alaska coast and the semipermanent Pacific high pressure to the southwest of the California coast. The annual mean winds for 2005 are northwesterly, approximately parallel to the central California coastline (Figure 1a), due to the influence of the Pacific high. The windspeed is characterized by a maximum near the coast and decreases with increasing offshore distance and is generally larger at higher latitudes. Strong variations in windspeed are evident along the coastline, characterized by five primary windspeed maxima located to the south of prominent capes and coastal topography, namely, Cape Blanco, Cape Mendocino, Point Arena, Point Sur, and Point Conception. Throughout this paper, we use the term offshore area to refer to the areas over the ocean and within the distance of approximately 100 km from the coastline. Between each pair of adjacent wind maxima, there is a windspeed minimum, located to the north of the coastal promontories, associated with terrain blocking. The windspeed in these offshore maxima is substantially stronger than over the open ocean, implying a significant enhancement by the marine boundary layer (MBL) and coastal terrain effects. The maximum windspeed zones extend approximately 50 km offshore, indicative of significant wind energy potential off the California coast. The standard deviation of the windspeed exhibits spatial variations similar to the windspeed with largest variations coincident with

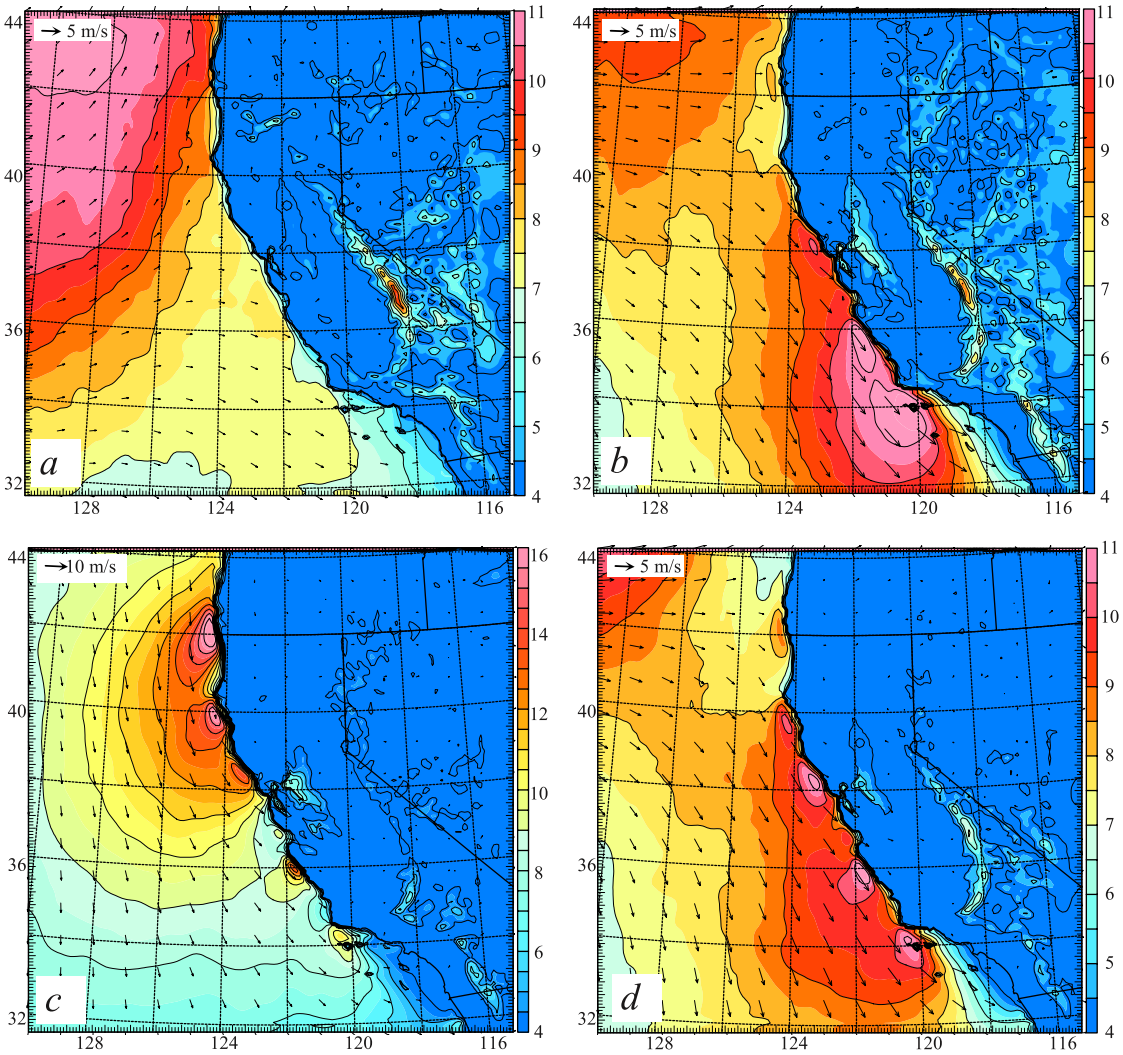

Figure 2. Monthly mean windspeed (color, increment: 0.5 m s^{-1}; contour, interval: 1 m s^{-1}) and wind vectors at 90 m AGL for (a) January, (b) April, (c) July, and (d) October, 2005.

the windspeed maxima in Figure 1a, suggesting that any change in large-scale winds is likely amplified in the offshore areas through MBL-terrain interaction (Figure 1b).

[8] The monthly mean winds for 2005 are shown in Figure 2, for January, April, July, and October, which are representative of the winter, spring, summer, and autumn months, respectively. During the winter months, the low-level winds are predominately southwesterly (northwesterly) offshore of northern (southern) California (Figure 2a) and the terrain effect is much less pronounced. In the spring months, the prevailing winds along the California coast are northwesterly (Figure 2b), and the terrain effect is more dramatic along the southern California coast. During the summer months, due to the strong Pacific high, the prevailing winds are northerly or northwesterly, nearly parallel to the California coastline. The interaction between MBL and coastal topography results in alternation of windspeed maxima and minima in the offshore zones (Figure 2c). It is evident that the five windspeed maxima are still present in the autumn months (Figure 2d). However, as the Pacific high is weaker and is positioned farther south than in the summer months, the windspeed is stronger offshore of southern California. Vertical cross-sections through the surface wind maxima indicate that in summer the strongest terrain enhancement occurs within the low-level jet typically residing at the MBL top inversion (Figure 3a). The MBL windspeed reaches a maximum just a few kilometers away from the coastline and decays slowly with the offshore distance (Figure 3a). The along-wind dimension of the windspeed maximum zone, typically comparable to the along-wind scale of the topography, is of the order of 100-km for the Cape Blanco maximum (Figure 3b).

[9] The interaction between the MBL and coastal terrain has been the subject of numerous studies [e.g., *Dorman et al.*, 1999; *Haack et al.*, 2001]. In the presence of a shallow MBL capped by an inversion, the surface wind maxima downstream of major capes, often referred to as expansion fans, can be readily interpreted using shallow water theory in terms of a supercritical flow past an obstacle. The MBL flow is often supercritical relative to the shallow-water wave speed ($\sqrt{g'H}$, where $g' = g\Delta\theta/\bar{\theta}$ is the reduced gravity, $\Delta\theta$ is the potential temperature difference across the MBL top inversion, $\bar{\theta}$ is the mean potential temperature in the MBL, and g is the gravity), i.e., $U/\sqrt{g'H} > 1$, where U is the mean

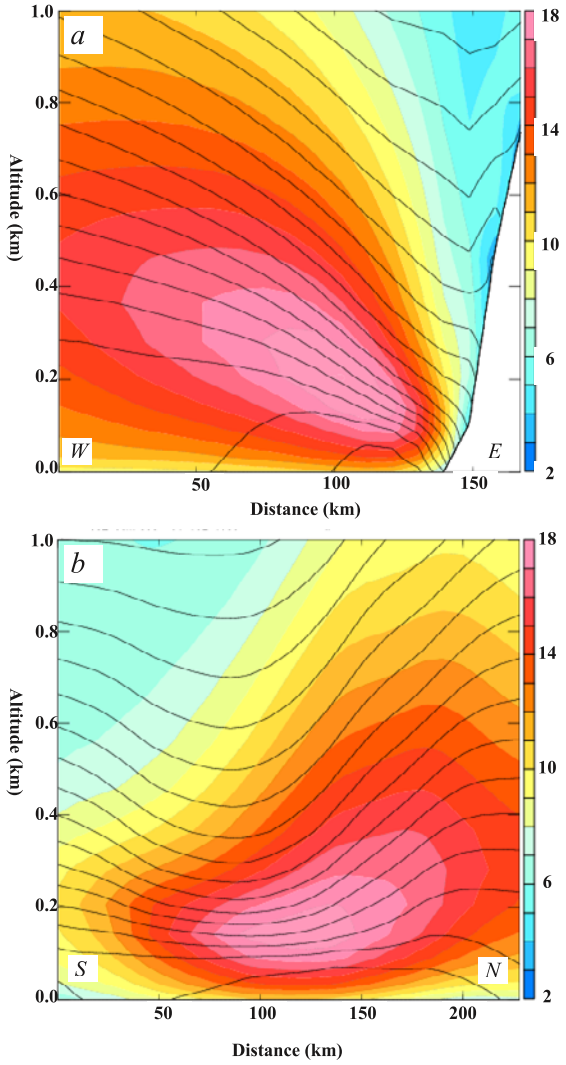

Figure 3. Vertical cross-sections of annual mean windspeed (color, interval: 1 m s^{-1}) and potential temperature contour (interval: 1 K) for the month of July 2005, through the Cape Blanco maximum and oriented (a) across the coastline and (b) along the coastline respectively (see Figure 1b for locations). The mean wind direction is out of page in Figure 3a and towards the left (south) in Figure 3b.

windspeed in the MBL. In a vertical section across the expansion fan axis oriented along the mean wind, the MBL first experiences a gentle expansion and then a contraction (Figure 3b), and the MBL flow is decelerated and accelerated accordingly following mass conservation. This dynamical response of the MBL to variations in the coastal topography is the primary factor in producing the dramatic spatial variability in the low-level windspeed for the late spring, through early autumn period.

4. Offshore Wind Power Potential Assessment

[10] To illustrate the significance of the coastal wind maxima, we examine characteristics of the low-level winds and assess the wind energy potential at two offshore windspeed maxima near Cape Blanco and Pt. Arena. Substantial seasonal variations of monthly mean winds at the two sites are evident (Figure 4). The windspeed peaks during the summer months when the coastal terrain effect is most significant, coinciding with the peak power demand period in California [*Price and Cable*, 2001]. At Cape Blanco, the MBL is shallower with stronger BL top inversion than at Point Arena during the summer months associated with a colder sea surface temperature, and consequently the winds at Cape Blanco are much stronger than at the Pt. Arena site. In the spring and fall months, the windspeed is stronger at Pt. Arena than at Cape Blanco.

[11] The windspeed frequency distribution can be approximated using the Weibull distribution function [*Weibull*, 1951],

$$f(v) = \frac{k}{c}\left(\frac{v}{c}\right)^{k-1} \exp\left[-(v/c)^k\right], \quad (1)$$

where $f(v)$ is the probability density function for windspeed v, c is the Weibull scale parameter, and k is the nondimensional shape parameter or slope. The two parameters can be determined from the mean windspeed, $\bar{v}$, and the standard deviation, σ, using $k = (\sigma/\bar{v})^{-1.086}$ and $c = \bar{v}/\Gamma(1 + 1/k)$, where Γ represents the Gamma function. The operating probability, i.e., the probability of the windspeed between the cut-in wind speed (minimum windspeed for a wind turbine to operate, v_{ci}) and cut-out wind speed (maximum windspeed above which the wind turbine should be turned off for equipment protection, v_{co}) is given by

$$p_o = \exp\left(-(v_{ci}/c)^k\right) - \exp\left(-(v_{co}/c)^k\right). \quad (2)$$

[12] Here we use the following empirical equation to estimate the energy output [*Jacobson and Masters*, 2001],

$$P = C \times P_{rated}(kW) \times 8760(hr/year), \quad (3)$$

where the capacity factor $C = 0.087\bar{v}(m/s) - P_{rated}(kW)/D(m)^2$, P_{rated} is the rated power and D is the blade diameter. The annual specific yield is given by $4P/(\pi D^2)$. The annual mean windspeed, standard deviation, Weibull distribution

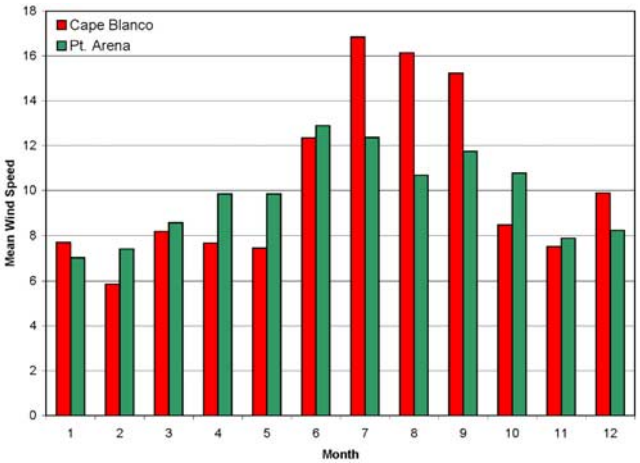

Figure 4. Histogram of the monthly mean windspeed for 2005 at the 90-m level offshore of Cape Blanco and Point Arena (see Figure 1b for locations).

Table 1. Annual Mean Windspeed, Standard Deviation, Operating Probability for v_{ci} = 4 m s^{-1}, and v_{co} = 25 m s^{-1}, Parameters for Weibull Distribution[a]

Altitude (m)	Annual Mean (m/s)	Standard Deviation (m/s)	Operating Probability (%)	Shape Parameter	Scale Parameter	Power Output (TWh)	Annual Specific Yield (KWh/m^2)
			Cape Blanco (Offshore)				
10	7.80	4.60	73	1.77	8.76	15.9	1276
50	9.50	5.85	78	1.69	10.63	22.4	1796
90	10.29	6.65	79	1.61	11.5	25.4	2037
			Point Arena (Offshore)				
10	7.29	3.69	77	1.78	8.23	14.0	1123
50	8.93	4.67	83	1.76	10.1	20.2	1620
90	9.78	5.35	84	1.66	11.0	23.5	1884

[a]Included are the k parameter and scale parameter. Also included are the annual energy output and annual specific field from a commercially available wind turbine with D = 126 m and P_{rated} = 5 MW at the two offshore sites near Cape Blanco and Point Arena.

parameters, operating probability, wind power density at Cape Blanco and Pt. Arena are listed in Table 1. The mean windspeed, standard deviation, scale parameter, operating probability, and output energy increase with the altitude near the surface. The distribution shape factor is between 1.6 and 1.8, less than two, suggesting that the frequency distribution of the windspeed in this area is more widespread than often-used Raleigh distribution ($k = 2$). The smaller shape factors are consistent with the relatively large standard deviations of the windspeed, implying that variations in large-scale flows are likely amplified through MBL-terrain interaction. The operating probabilities for the two offshore sites are around 80%.

[13] As an example, consider a wind farm consisting of a network of wind turbines as specified in Table 1 with an inter-turbine spacing of $4D \times 7D$, where $D = 126\ m$ is the blade diameter. Approximately 10000 such wind turbines could be installed in the area offshore of Cape Blanco where the climatological wind speed maximum occurs (Note: Bathymetry and potential exclusions are not considered here). Using the 90-m average power output from Table 1, the total power generated by a network of these wind turbines is ~29000 MW, approximately 35% of the total electrical energy generation in California in 2006 (http://www.energyalmanac.ca.gov/electricity/electricity_generation.html).

5. Conclusions

[14] In this study, the spatial and temporal variations of low-level winds and the associated wind energy potential offshore of the California coast have been examined using a well-tested model dataset. Along the California coast, the low-level windspeed exhibits strong spatial variations, characterized by five primary windspeed maxima located downstream of major capes: Cape Blanco, Cape Mendocino, Point Arena, Point Sur, and Point Conception. The five windspeed maxima extend approximately 50 km offshore, and are evident in the annual mean windspeed and windspeed standard deviation fields, underscoring the strong impact of the marine boundary layer-terrain interaction on near-surface winds offshore of California.

[15] An analysis indicates that the terrain effect is least significant during the winter months. The mean windspeed along the California coast increases with the latitude associated with the frontal activity in the winter to early spring months. The influence of MBL-terrain interaction on low-level winds is most significant during the summer months in the presence of a well-defined MBL associated with the Pacific high positioned to the southwest of the California coast. In the spring and late fall months, the influence of the Pacific high is confined to the southern California coast. Accordingly, the low-level winds are generally stronger offshore of the southern California coast. The alternation of windspeed maxima and minima along the coastline can be interpreted using hydraulic theory, especially for the late spring through early fall period.

[16] The windspeed at the two offshore sites near Cape Blanco and Pt. Arena exhibits strong seasonal variations, characterized by larger windspeed during the summer months and weaker windspeed during the winter months, which is in phase with the seasonal cycle of the California power demand. The results of this study highlight the enormous reliable wind power potential offshore of the California coast, particularly downwind of coastal promontories.

[17] **Acknowledgments.** This research was supported by the Office of Naval Research (ONR) program element 0601153 N. The first author has greatly benefited from discussions with Ronald Smith at Yale University. COAMPS is a registered trademark of the Naval Research Laboratory.

References

Archer, C. L., and M. Z. Jacobson (2005), Evaluation of global wind power, *J. Geophys. Res.*, *110*, D12110, doi:10.1029/2004JD005462.

Capet, X. J., P. Marchesiello, and J. C. McWilliams (2004), Upwelling response to coastal wind profiles, *Geophys. Res. Lett.*, *31*, L13311, doi:10.1029/2004GL020123.

Dorman, C. R., D. P. Rogers, W. Nuss, and W. T. Thompson (1999), Adjustment of the summer marine boundary layer around Point Sur, California, *Mon. Weather Rev.*, *127*, 2143–2159.

Doyle, J. D., Q. Jiang, Y. Chao, and J. Ferrara (2008), High-resolution atmospheric modeling over the Monterey Bay in support of the AOSNII field campaign, *Deep Sea Res. Part II*, in press.

Elliot, D. L., and M. N. Schwartz (1998), Validation of regional wind resource predictions in the northern Great Plains, paper presented at Windpower 1998, Am. Wind Energy Assoc., Bakersfield, Calif.

Haack, T., S. D. Burk, C. Dorman, and D. Rogers (2001), Supercritical flow interaction within the Cape Blanco-Cape Mendocino orographic complex, *Mon. Weather Rev.*, *129*, 688–708.

Hasager, C. B., M. Nielsen, P. Astrup, R. Barthelmie, E. Dellwik, N. O. Jensen, B. H. Jorgensen, S. C. Rathmann, and B. R. Furevik (2005), Offshore resource estimation from satellite SAR wind field maps, *Wind Energy*, *8*, 413–419.

Hodur, R. M. (1997), The Naval Research Laboratory's Coupled Ocean/Atmospheric Mesoscale Prediction System (COAMPS), *Mon. Weather Rev.*, *125*, 1414–1430.

Jacobson, M. Z., and G. M. Masters (2001), Exploiting wind versus coal, *Science*, *293*, 1438.

Musial, W., and S. Butterfield (2004), Future of offshore wind energy in the United States, report, Natl. Renewable Energy Lab., Dep. of Energy, Golden, Colo.

Price, H., and R. Cable (2001), Parabolic trough power for the California competitive market, presented at 2001 Solar Energy Forum: The Power to Choose, Natl. Renewable Energy Lab., Dep. of Energy, Washington, D. C.

Weibull, W. (1951), A statistical distribution function of wide applicability, *J. Appl. Mech.*, *18*, 293–297.

C. L. Archer, Department of Geological and Environmental Sciences, California State University - Chico, Chico, CA 95929, USA.

J. D. Doyle and T. Haack, Naval Research Laboratory, Monterey, CA 93943-5502, USA.

M. J. Dvorak and M. Z. Jacobson, Department of Civil and Environmental Engineering, Stanford University, Stanford, CA 94305-4020, USA.

Q. Jiang, University Corporation for Atmospheric Research, Naval Research Laboratory, Monterey, CA 93490-5502, USA. (qingfang.jiang@nrlmry.navy.mil)